

PATIENT DOSE STUDY IN CHEST RADIOGRAPHIC EXAMINATIONS FOR DIFERENT EXPOSURE TECHNIQUES USING MONTE CARLO METHODS AND VOXEL PHANTOM

**Samanda C. A. Correa¹, Edmilson M. Souza¹, Ademir X. Silva², Hélio Yoriyaz³,
Ricardo T. Lopes¹**

¹[Programa de Engenharia Nuclear]/COPPE, Universidade Federal do Rio de Janeiro
Ilha do Fundão, Caixa Postal 68509, 21945-970, Rio de Janeiro, RJ, Brasil
scorea@con.ufrj.br
emonteiro@con.ufrj.br
ricardo@lin.ufrj.br

²[PEN/COPPE - DNC/Poli]CT, Universidade Federal do Rio de Janeiro
Ilha do Fundão, Caixa Postal 68509, 21945-970, Rio de Janeiro, RJ, Brasil
ademir@con.ufrj.br

³[Instituto de Pesquisas Energéticas e Nucleares]/CNEN
Av. Lineu Prestes, 2242 – Cidade Universitária
Armando Salles Oliveira Pinheiros
Caixa Postal 11049, 05422-270, São Paulo, SP, Brasil
hyoriyaz@ipen.br

ABSTRACT

Monte Carlo code MCNPX coupled with an adult voxel female model (FAX) were used to investigate how radiation dose in chest radiographic examinations vary with antiscatter techniques (air gap and grid) and projection geometry (anterio-posterior – AP and posterio-anterior – PA) for different tube voltages. The radiation doses were evaluated in terms of organ and effective doses, for a fixed air kerma at the image detector. The results show that the effective dose for grid technique decreases with increasing tube voltage, while that for air gap great variations were not observed. Besides, the work also showed that doses are larger for AP projections and that use of the air gap is recommended in the place of the anti-scatter grids.

1. INTRODUCTION

Chest radiography is the most frequent tool in medical diagnostic examination for allowing the evaluation of a very wide range of clinical complaints [1]. However, radiation exposure can not be assumed to be purely beneficial. X-rays are capable of stripping electrons from atoms to form substances that are highly reactive in a chemical sense. Molecular bonds between atoms can be broken, and if this occurs within the nucleus of a cell in the body it can lead to irreparable damage, with long-term consequences for the viability or correct functioning of the cell. For this is important that radiological examinations performed are justified and optimized. To justify radiological examinations, risks to the patient from the radiation exposure should be known. Although the knowledge of the organ doses is important, these can not be measured directly inside patients. For this reason it is important to establish ways to study organ doses.

Monte Carlo code MCNP has been widely accepted as one of the most accurate tool for calculating dose distributions. MCNP is a general purpose transport code that can be used for

neutron, photon and electron or coupled particle transport. It has the capability of easily inputting complex geometry in three dimensions making the code very user friendly. Moreover, it has a wide range of capabilities for medical physics applications, mainly when used voxel phantom.

Kramer et al. [2] has developed an adult voxel female model (FAX) phantom based on CT images of female patients, whose organ and tissue masses have been adjusted in order to correspond to the anatomical specifications defined by the ICRP Publication 89 for the Female Reference Adult [3]. This new phantom connected to the Monte Carlo code MCNPX⁽⁴⁾ come as a great alternative in the study of parameters that can affect the dose in medical applications.

The objective of this work is to use the above-mentioned Monte Carlo code MCNPX and the FAX voxel phantom to provide the organ and effective doses in chest exams. These quantities will be studied for different tube voltages, projection geometry (anterio-posterior – AP and postero-anterior – PA) and antiscatter techniques (air gap and grid) for a fixed air kerma at the image detector of 5 μ Gy.

2. MODELED SYSTEM

2.1. Computer model

The calculations were made using a Monte Carlo code MCNPX version 2.5.0 [4]. The imaging system was modeled by simulating photon transport from the x-ray tube and through the patient and anti-scatter device. The photons were transported taking into account photoelectric absorption, coherent and incoherent scattering. Each calculation was based on generation 10^8 photons. The relative statistical errors were less than 0.05 for energy deposition, except for ovaries and bladder where was accepted a relative statistical error less than 0.1.

2.2. X-ray source

The initial photon energy was sampled from an x-ray spectrum pre-calculated with a program by Cranley et al. [5], which uses the tube peak voltage, anode material, filter material and filter thickness as input parameters. The energy distributions of x-ray used were obtained using 5.0 mm aluminum (Al) filtration and tungsten anode material. X-ray photons were emitted from a focal point with 3 mm diameter and a lead collimation was used to obtain a field size of 33 x 29 cm^2 in the phantom skin.

2.3. Voxel phantom

The voxel phantom FAX [2] was used as a model of a patient. The FAX is 163 cm height and has a mass of 59.76 kg. It was modeled in MCNPX code utilizing the SCMS software [6], which is a computational tool for the construction of geometric or anatomic models from medical images like Computerized Tomography (CT), Single Photon Emission Computerized Tomography (SPECT) or other similar digital images. The SCMS software interprets the images and provides an input file to be used by the Monte Carlo MCNPX code for the simulation of the radiation transport [7].

2.4. Antiscatter techniques and irradiation setup

Two different antiscatter techniques were studied, the antiscatter grid and the air gap. In the first technique a linear focused grid was modeled. The interspace and the front and back covers of the grid were composed of aluminum (Al); the radiopaque strips were made of lead (Pb). The parameters of the grids included in this study are listed in Table 1.

Table 1. Grid parameters.

Strip density (lines/cm)	Thickness of aluminum cover (μm)	Thickness of lead strips (μm)	Thickness of aluminum interspace (μm)	Lead-to-interspace ratio	Grid ratio
33	400	50	250	1/5	12

The validation of the grid was made by calculation of transmission of total (Tt), primary (Tp), bucky factor (BF) and contrast improvement factor (CIF) through the methodology and experimental measurements published by Chan et al. [8]. Table 2 compares simulated and measured values for studied grid.

Table 2. Comparison of measured and simulated grid performance parameters. The validation was made using the tube potential of 80 kV with filtration of 2.5 mm Al, water phantom with thickness of 20 cm, and a pair of Kodak lanex regular screens ($\text{Gd}_2\text{O}_2\text{S:Tb}$, 70 mg/cm^2 per screen).

Simulate Values				Experimental measurements from Chan et al.			
Tt	Tp	BF	CIF	Tt	Tp	BF	CIF
0.163	0.604	6.13	3.70	0.159	0.581	6.29	3.65

The grid was placed after the voxel phantom, where the distance from the phantom to the grid was kept at 1.0 cm. The focal-spot-to-grid distance was 151 cm, equal to the focal length of the grid studied. In the air gap technique a focal-spot-to-detector distance of 300 cm was used with 30 cm of separation distance between the phantom and the detector. With these irradiation setups, chest exposures with postero-anterior (PA) and antero-posterior (AP) projections were evaluated and effective dose and absorbed dose were obtained using 72-150 kV voltage tube range.

2.5. Dose calculation

The effective dose was calculated as the sum of the average absorbed doses in the individual organs multiplied by the appropriate tissue-weighting factors from ICRP Publication 60[9]. For each technique the doses were normalized to an air kerma at the image detector of 5.0 μGy , corresponding to a sensitivity class of 200 at the automatic exposure control (AEC) chambers [10].

The doses were measured in terms of the air kerma at the image detector in order to assure that, independent of the employed technique, the same conditions of exposure at the detector would be maintained to obtain the radiographic images.

3. RESULTS

The Figures 1 (a) and (b) show the effective dose as a function of tube voltage for PA (a) and AP (b) projections using grid and air gap techniques. Compared the Figure 1 (a) and (b) can be observed that the effective dose for AP projection is larger than PA projection; yet, the difference is very larger for air gap. This occurred due to a larger number of organs present higher doses for AP projection with air gap than grid, as shown in the Figure 2 (a) and (b). In the Figure 2 can also verify the high values of doses from breast and thyroid for AP projection, as a result of the positioning of those organs for the irradiation configuration.

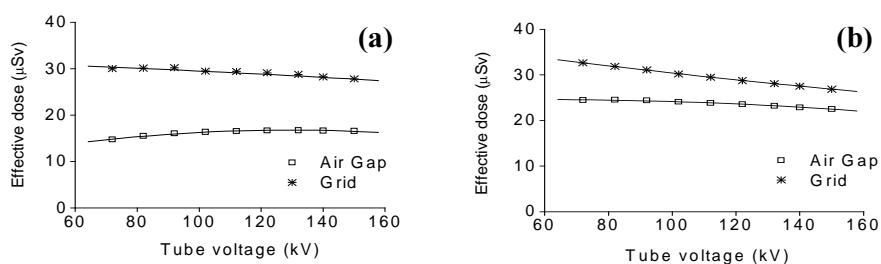


Figure 1. The effective dose as a function of tube voltage for grid and air gap techniques. In (a) PA projection, and (b) AP projection.

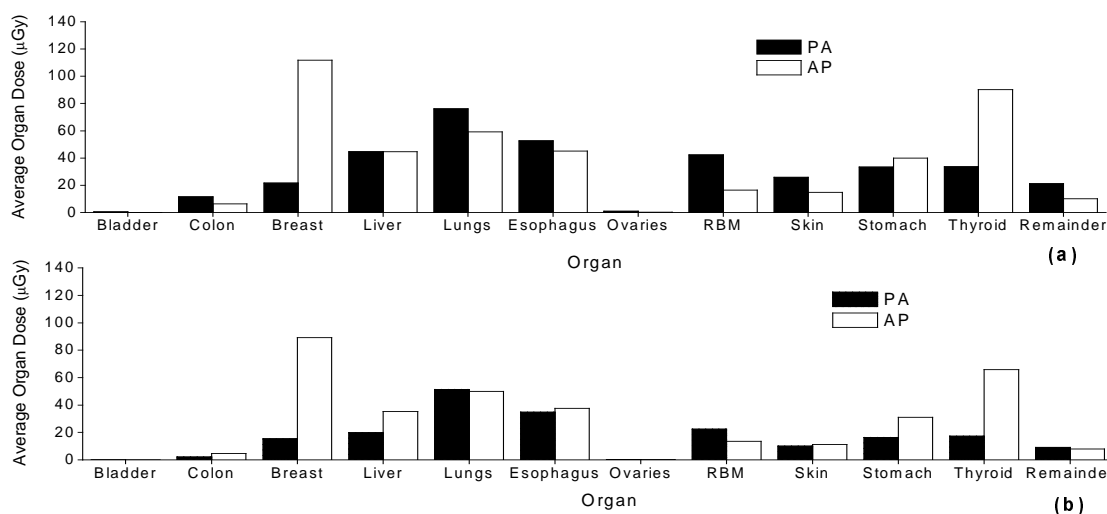


Figure 2. Average organ dose for PA and AP projections obtained with 102 kV tube voltage. In (a) grid technique, and (b) air gap technique. The doses of the bladder and ovaries can not be observed in the graph due to the low values. Those organs presented low doses because they were not irradiated directly and due to the small size.

Through the Figures 1 (a) and (b) are also observed that using a grid, the effective dose decreases slowly with increasing tube voltage. The decrease is about 29% for PA projection and 30% for AP projection, and it occurs due to higher grid transmission at high photon energies [10]. In contrast, for air gap technique, the effective dose is fairly constant with tube voltage. The variation is approximately 11% for PA projection and 8% for AP projection.

The analyzed data in Figure 1 also show that the doses are higher when obtained with grid for both studied projections. For PA and AP projections the doses obtained with the grid are about 45% and 20% higher than obtained with air gap, respectively. Likewise, the average dose in the radiosensitive organs is also larger for grid in both studied projections as shown in

the Figures 3 and 4. In these Figures can also be verified that the largest value of absorbed dose for PA projection was to lung and for AP projection to breast and thyroid, independent of the antiscatter technique. Besides, the doses in those organs also present a soft decreasing behavior as a function of the tube voltage when grid is used. For air gap, this behavior is only observed for breast and thyroid for AP projection. In the grid technique, as sees previously, there is a higher grid transmission at high photon energies what causes the observed behavior. For air gap the decrease of the doses in the breast and thyroid with the tube voltage occurs due a stronger dose gradient from the entrance surface of the phantom for low tube voltage. In a higher tube voltage the dose distribution will be more uniform.

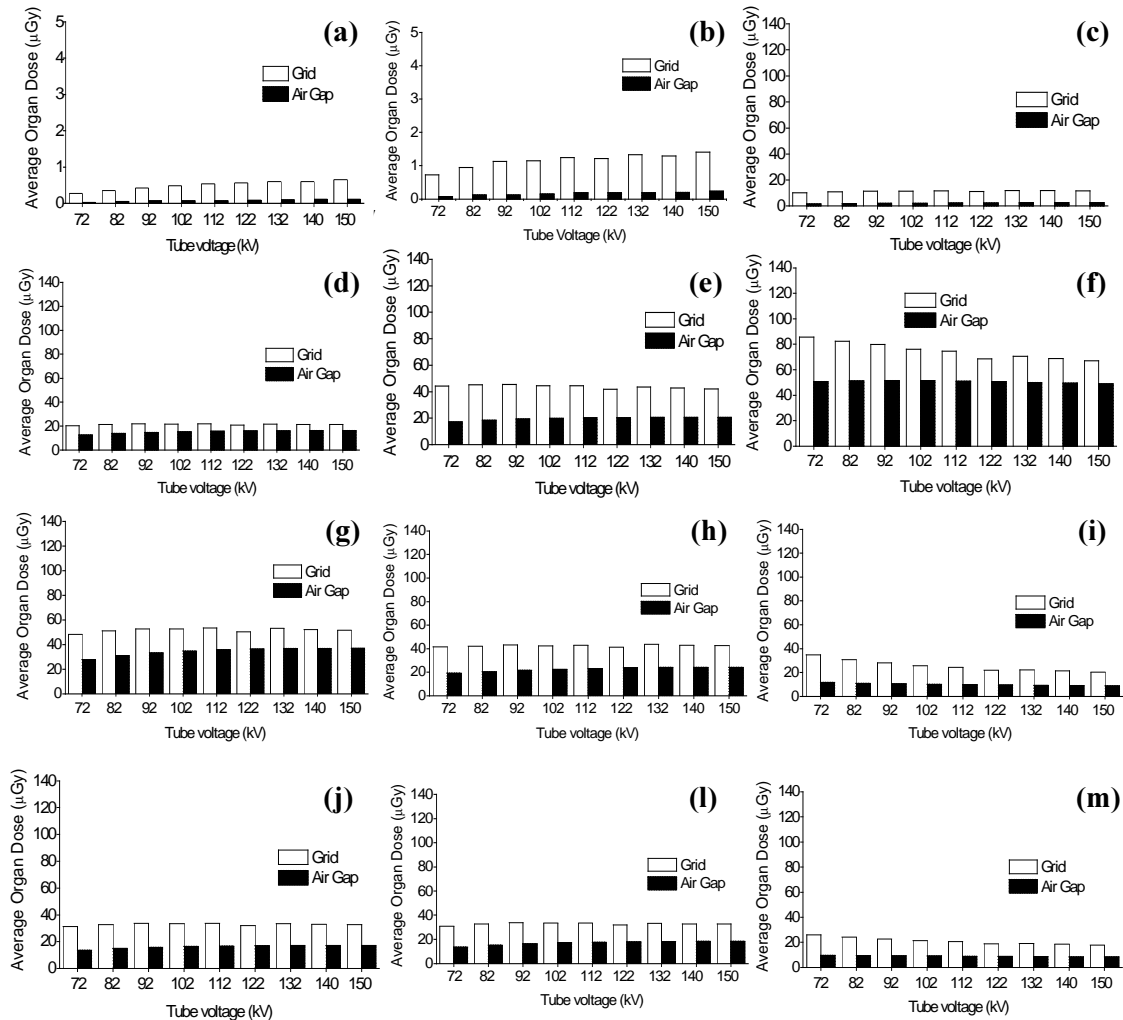


Figure 3. Average organ dose as a function of tube voltage for grid and air gap techniques with PA projection. In (a) bladder, (b) ovaries, (c) colon, (d) breast, (e) liver, (f) lungs, (g) esophagus, (h) red bone marrow, (i) skin, (j) stomach, (l) thyroid, (m) remainder.

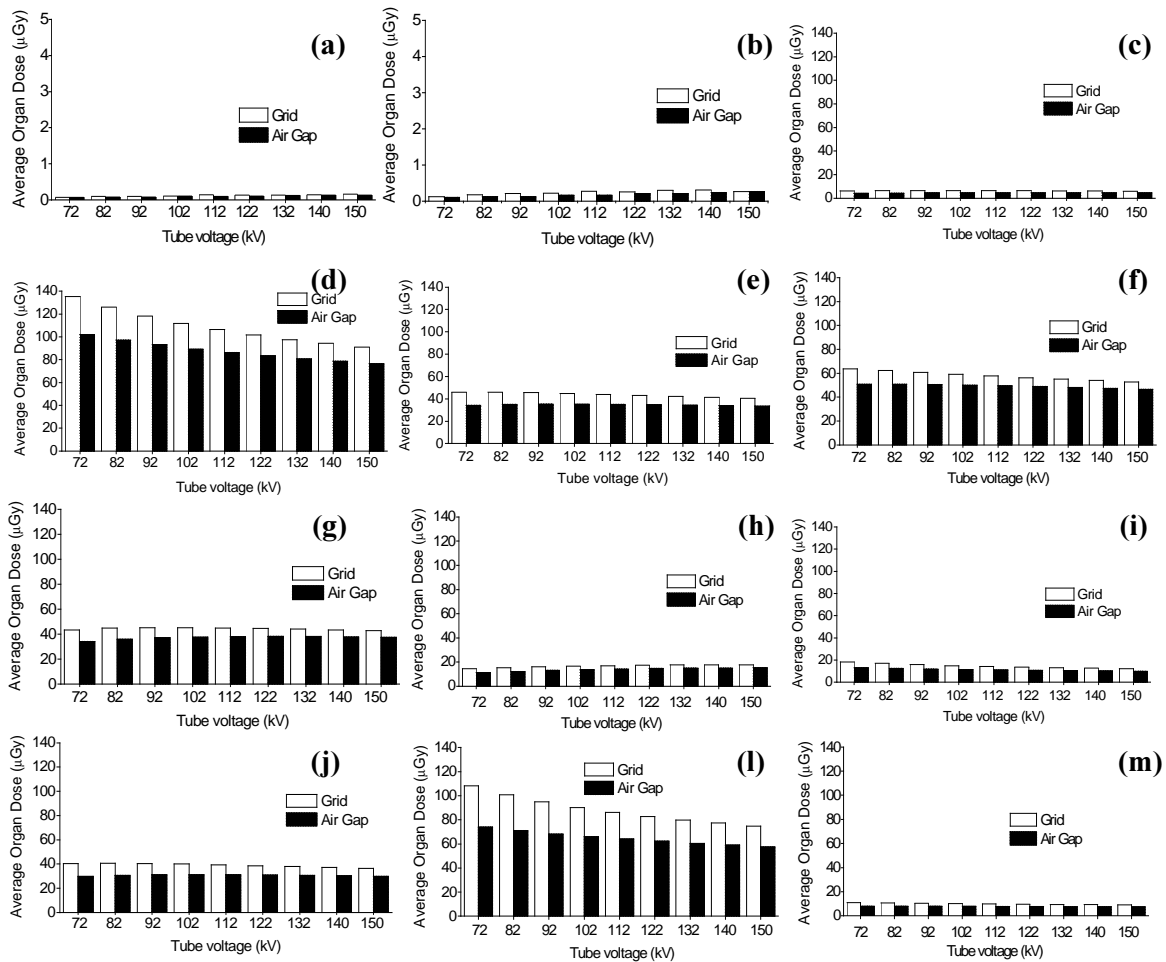


Figure 4. Average organ dose as a function of tube voltage for grid and air gap techniques with AP projection. In (a) bladder, (b) ovaries, (c) colon, (d) breast, (e) liver, (f) lungs, (g) esophagus, (h) red bone marrow, (i) skin, (j) stomach, (l) thyroid, (m) remainder.

4. DISCUSSION

In this study, for purpose of radiation protection, the radiation doses received from chest exams were evaluated. The present analysis showed that the obtained doses with the grid technique are larger than with the air gap for both evaluated geometric projections (AP and PA). Besides, the work also showed that obtained effective doses in AP projection are larger when compared with PA projection, and that these doses using grid technique decreases with increasing tube voltage. For air gap technique this behavior was approximately constant.

Similar results were also found by Lloyd et al. [11] and Bell et al. [12] for fluoroscopic and lateral cervical spine examinations. They demonstrated that the removal of the grid reduced the dose in the patient. Furthermore, more studies support the results of this work, Lee et al. [13] showed that the doses in chest and abdomen x-ray exams with AP projection are larger than with PA projection, and Ullman et al. [10] verified that using grid the effective dose decreases with increasing tube voltage due to higher grid transmission at high photon energies, while that for air gap great variations were not observed.

Other works in the literature have also been encouraged the changes in working procedures for chest exams. Lannhede et al. [14] performance a clinical trial in which different imaging system configurations for the chest PA examination were compared. In this trial patient images were evaluated by a group of expert radiologists using the EC image criteria [15]. Comparing the anti-scatter techniques they had concluded that the best image quality and the smallest dose were obtained using the air gap system. Similar resulted it was also found for Hwang [16] for analogical systems and Ullman et al [10] in digital chest radiography.

5. CONCLUSION

The results of this study encourage changes in the working procedures for chest exams. The use of the air gap should be incorporated in the place of the anti-scatter grids as dose reduction strategy for the patient. Those results also confirm that the Monte Carlo code MCNPX coupled to FAX voxel phantom are useful in dosimetric studies in medical diagnostic examination.

ACKNOWLEDGEMENTS

The authors wish to thank the financial support of the Conselho Nacional de Desenvolvimento Científico e Tecnológico (CNPq) and Fundação Carlos Chagas Filho de Amparo à Pesquisa do Estado do Rio de Janeiro (FAPERJ), Brazil.

REFERENCES

1. International Commission on Radiation Units and Measurements. "Image Quality in Chest Radiography". *ICRU Report 70* (2003).
2. Kramer, R., Houry, H. J., Vieira, J. W., Loureiro, E. C. M., Lima, V. J. M., Lima, F. R. A., Hoff, G. "All about FAX: a female adult voxel phantom for Monte Carlo calculation in radiation protection dosimetry". *Phys. Med. Biol.* Vol. 49, pp. 5203-5216 (2004).
3. International Commission on Radiological Protection. "Basic Anatomical and physiological data for use in radiological protection: reference values". *ICRP Publication 89* (Oxford: Pergamon Press) (2003).
4. Pelowitz, D. B. "MCNPXTM User's Manual", Version 2.5.0. LA-CP-05-0369. *Los Alamos National Laboratory* (2005).
5. Cranley, K., Gilmore, B. J., Fogarty, G. W. A., Desponds, L. "Catalogue of diagnostic x-ray spectra and other data". *The Institute of Physics and Engineering in Medicine*, Report 78 (1997).
6. Yoriyaz, H., Santos, A., Stabin, M. "Absorbed Fractions in a Voxel-Based Phantom Calculated with the MCNP-4B Code". *Med. Phys.* Vol. 27(7), pp. 1555-1562 (2000).
7. Yoriyaz, H., Stabin, M., Santos, A. "Monte Carlo MCNP-4B Based Absorbed Dose Distribution Estimates for Patient – Specific Dosimetry". *J. Nuc. Med.* Vol. 42(4), pp. 662-669 (2001).
8. Chan, H.P., Higashida, Y., Doi, K. "Performance of Antiscatter grids in Diagnostic Radiology: Experimental Measurements and Monte Carlo Simulation Studies". *Med. Phys.* Vol. 12(4), pp. 449-454 (1985).
9. International Commission on Radiological Protection. "Recommendations of the International Commission on radiological protection". *ICRP Publication 60* (Oxford: Pergamon Press) (1991).

10. Ullman, G., Sandborg, M., Dance, D.R., Hunt, R.A., Carlsson, G.A. "Towards Optimization in Digital Chest Radiography using Monte Carlo Modelling". *Phys. Med. Biol.* Vol. 51, pp. 2729-2743 (2006).
11. Lloyd, P., Lowe, D., Harty, D.S., Eyes, B. "The Secondary Radiation Grid; Its Effect on Fluoroscopic Dose-Area Product During Barium Enema Examinations". *The British Journal of Radiology* Vol. 71, pp. 303-306 (1998).
12. Bell, N., Erskine, M., Warren-Forward, H. "Lateral Cervical Spine Examinations: An Evaluation of Dose for Grid and Non-grid Techniques". *Radiography* Vol. 9, pp. 43-52 (2003).
13. Lee, S. C., Wang, J. N., Liu, S. C., Jiang, S. H. "Effective dose evaluation for chest and abdomen x-ray tests". *Radiat. Prot. Dosim.* Vol. 116, pp. 613-619 (2005).
14. Lanhede, B., Tinberg, A., Mansson, L. G., Kheddache, S., Widell, M., Björnelid L., Sund, P., Almen, A., Besjakov, J., Mattsson, S., Zankl, M., Panzer, W., Herrmann, C. "The influence of different technique factors on image quality for chest radiographs: Application of the recent CEC image quality criteria". *Radiat. Prot. Dosim.* Vol. 90, pp. 203-206 (2000).
15. Carmichael, J.H., Maccia, C., Moores, B.M., Oestmann, J.W., Schibilla, H., Van Tiggelen, R., Wall, S. "European guidelines on quality criteria for diagnostic radiographic images". *Report EUR 16260 EN*, European Commission, Luxembourg (1996).
16. Hwang, S. F. "Otimização da qualidade e da dose em radiologia geral do tórax". *Dissertação de Mestrado*. Departamento de Biofísica da Universidade Federal de Pernambuco (2001).